Localization for correlated binary-alloy disorder

E. N. Economou
Exxon Research and Engineering Company, Annandale, New Jersey 08801
and Research Center of Crete, P.O. Box 1527, Heraklio, Crete, Greece

C. M. Soukoulis* and M. H. Cohen
Exxon Research and Engineering Company, Annandale, New Jersey 08801
(Received 5 February 1987)

A one-dimensional tight-binding model with correlated binary-alloy disorder is studied both numerically and analytically. The dependence of the localization length on the correlation parameter is determined for various energies and impurity correlations. The results are compared with the predictions of the quasiuniversality idea recently developed by the authors.

I. INTRODUCTION

Although the problem of disorder and localization has been studied extensively[1-3] over the last 20 years, most of the theoretical work has been confined to simple tight-binding models, where the diagonal matrix elements ε_n of the Hamiltonian are *independent* random variables. The question of statistically correlated diagram matrix elements has been examined mainly in connection with extensions of the coherent-potential approximation[4,5] and the problem of magnetic ordering.

Recently, we have demonstrated[6] that, when no other relevant length is comparable to or smaller than the potential correlation length L, certain aspects of the problem reduce to those of a white-noise model and, as a result, a certain quasiuniversality (QU) energies. The latter allows a determination of the dependencies on L, w^2, m^* from dimensional considerations; w^2 is the variance of any diagonal matrix element ε_n and m^* is the effective mass of the unperturbed Hamiltonian, which in terms of the tight-binding parameters is given by $m^* = \hbar^2/2Va^2$. The quantity V is the nearest-neighbor matrix element (which we take as constant) and a is the lattice spacing.

The reduction to the white-noise problem and the quasiuniversality which emerges from it is very important, because it allows—within its limits of validity—a simple and general treatment of the disordered band, in a similar way that the effective mass simplifies the treatment of a periodic band. For this reason it is very important to find out the domain of approximate validity of the QU. We have already shown that for a single-band tight-binding model with no off-diagonal disorder (i.e., V constant) and no correlation among the different diagonal matrix elements, the QU is reasonably valid up to disorder w about equal to 20% of the bandwidth and for energies (measured from the nearest band edge) up to about 20% of $|E_B - E_{\rm VH}|$, where E_B is the band edge and $E_{\rm VH}$ is the energy of the nearest van Hove singularity. The presence of off-diagonal disorder violates the QU; however, the violation tends to be small in most cases. In the present paper we would like to check the validity of the QU in the presence of correlations between the atomic potentials, i.e., under which circumstances and to what extent the potential correlation length L can simply replace the lattice spacing a in our uncorrelated results. Furthermore, finding the effects of potential correlations on transport and localization properties is a very interesting problem in its own right, since these effects are far from obvious; indeed the traditional weak-scattering, long-wavelength approach to the transport problem implies that transport quantities such as the mean free path l must be proportional to the $-d$ power of the correlation length L, where d is the dimensionality. The argument is as follows: l^{-1} is proportional to the concentration of scattering centers times the cross section of each one.[3] The scattering cross section increases with L as L^{2d} (in the weak-disorder, long-wavelength limit), while the concentration decreases as L^{-d}. Thus $l \sim L^{-d}$. On the other hand, one may argue that increasing the correlation length effectively reduces the disorder (this is definitely true for very large L, since then the potential fluctuations tend to disappear). Hence, on the basis of that argument one would expect l to be an increasing and not a decreasing function of L. We shall see that both behaviors as well as intermediate ones appear depending on the energy, the amount and type of disorder, and on whether the scattering potential is attractive or repulsive.

In Sec. II we present our model, a single-orbital-per site, tight-binding, one-dimensional model with a correlated binary-alloy diagonal randomness and no off-diagonal disorder. The model has the important advantage of allowing explicit numerical calculations (presented in Sec. III) as well as some analytical results. Furthermore, it is very rich, incorporating many physically different circumstances. On the other hand, the one dimensionality and the binary character of the disorder strongly exaggerate certain effects of the correlation and constitute an extremely unfavorable combination for the validity of the QU. In Sec. IV we provide—through some analytical calculations—interpretation of and comments on our numerical results. Finally, in Sec. V we present our main conclusions.

 ©1988 The American Physical Society

II. THE MODEL AND THE PREDICTIONS OF THE QU

Our Hamiltonian H is given by

$$\langle m \mid H \mid n \rangle = \begin{cases} \varepsilon_n & \text{for } n=m \ , \\ V & \text{for } n=m\pm 1 \ , \\ 0 & \text{otherwise} \end{cases} \tag{2.1}$$

where $\mid n \rangle$, $\mid m \rangle$ are atomiclike orbitals centered at the n and m sites, respectively, of an infinite one-dimensional lattice of spacing a. The off-diagonal matrix element V is considered constant and is taken as our unity of energy. The quantities $\{\varepsilon_n\}$ are correlated random variables with a binary-alloy probability distribution which is characterized by three parameters ε, x, and p. The first two determine the probability distribution of any single variable,

$$p(\varepsilon_n)=x\delta\left[\varepsilon_n-\frac{\varepsilon}{2}\right]+(1-x)\delta\left[\varepsilon_n+\frac{\varepsilon}{2}\right] , \tag{2.2a}$$

and the third, p, specifies the correlation as follows:

$$p_{BA}=(1-x)p \ , \tag{2.2b}$$

where p_{BA} is the probability that two given consecutive sites have site energies $-\varepsilon/2$ and $\varepsilon/2$, respectively. We call a site A (B) if its ε_n has the value $\varepsilon/2$ ($-\varepsilon/2$). If $p=x$ the random variables $\{\varepsilon_n\}$ are uncorrelated. If $p<x$ the correlation is towards segregation, and at $p=0$ we have complete phase separation. Since the transformation $E\rightarrow -E$ and $x\rightarrow 1-x$ leaves all physical quantities invariant, we can, without loss of generality, assume that $x\leq 0.5$, which means that A is the minority constituent. We can easily show that

$$\langle \varepsilon_n \rangle = \varepsilon(x-\tfrac{1}{2}) \tag{2.3}$$

and

$$w^2 \equiv \langle (\varepsilon_n - \langle \varepsilon_n \rangle)^2 \rangle = \varepsilon^2 x(1-x) \ . \tag{2.4}$$

One can set up a difference equation which allows the determination of the probability $p_{n\,\alpha/\beta}$ that the n site is α ($\alpha=A$ or B) under the condition that the zero site is β ($\beta=A$ or B). For example,

$$p_{n\,A/B}=p_{n-1\,A/B}p_{A/A}+p_{n-1\,B/B}p \ , \tag{2.5}$$

where $p_{A/A}=1-p_{B/A}$ is the probability that a given site is A under the condition that a given neighbor is A. From Eq. (2.5) we obtain

$$p_{n\,A/B}=x-(x-p)\left[\frac{x-p}{x}\right]^{n-1} . \tag{2.6}$$

Similarly, we obtain

$$p_{n\,A/A}=x+\frac{(1-x)(x-p)}{x}\left[\frac{x-p}{x}\right]^{n-1} . \tag{2.7}$$

Note that, for $x<0.5$, p cannot reach unity, but it is less than $x/(1-x)$. The correlations decay exponentially with a characteristic length equal to $a/\ln(x/\mid x-p \mid)$. However, this is not the correlation length L appropriate to the QU argument. The proper definition of L for the continuum is

$$L^d=\frac{1}{w^2}\int d^dx \langle [V(x)-\langle V\rangle]/[V(0)-\langle V\rangle] \rangle \ . \tag{2.8}$$

In the present one-dimensional discrete case, the definition becomes

$$L=\begin{cases} \dfrac{a}{w^2}\displaystyle\sum_n \langle (\varepsilon_n-\langle\varepsilon_n\rangle)(\varepsilon_0-\langle\varepsilon_n\rangle)\rangle, & p\leq x \qquad (2.9a) \\ \dfrac{a}{w^2}\displaystyle\sum_n (-1)^n\langle (\varepsilon_n-\langle\varepsilon_n\rangle)(\varepsilon_0-\langle\varepsilon_n\rangle)\rangle, & x\leq p \ . \qquad (2.9b) \end{cases}$$

Note that $(-1)^n$ factor for the case of AB correlations. Using Eqs. (2.6) and (2.7) we find that

$$\langle (\varepsilon_n-\langle\varepsilon\rangle)(\varepsilon_0-\langle\varepsilon_n\rangle)\rangle = w^2\left[\frac{x-p}{x}\right]^{\mid n\mid} . \tag{2.10}$$

Substituting in (2.9a) and (2.9b) we obtain a very simple result

$$L/a=\begin{cases} \dfrac{2x-p}{p}, & p\leq x \qquad (2.11a) \\ \dfrac{p}{2x-p}, & p\geq x \ . \qquad (2.11b) \end{cases}$$

Thus L/a is always greater than or equal to 1. The equality is obtained in the absence of correlations, i.e., when $p=x$.

The QU argument[6] is based on the assumption (valid in the long-wavelength, weak-scattering limit) that there are only two relevant physical quantities: the quantity $\gamma=w^2L^d$, where w^2 is the variance of the randomly fluctuating potential and L is the correlation length within which the potential varies very little, and the effective mass m^*. From these quantities one uniquely defines (for $d\neq 4$) units of length L_{0d} and energy E_{0d} as follows:

$$L_{0d}=\hbar^{4/(4-d)}/\gamma^{1/(4-d)}m^{2/(4-d)} \ , \tag{2.12}$$

$$E_{0d}=m^{d/(4-d)}/\gamma^{2/(4-d)}/\hbar^{2d/(4-d)} \ . \tag{2.13}$$

The mean free path l, the localization length λ, or any other relevant length can then be expressed as

$$l/L_{0d}=f_d(E/E_{0d}) \ , \tag{2.14}$$

For E small, i.e., close to the band edge (which implies the long-wavelength limit) the function $f_d(x)$ behaves as $x^{(3-d)/2}$

$$f_d(x)\sim x^{(3-d)/2} \quad \text{for } 1\ll x \ll \hbar^2/2m^*L^2E_{0d} \ . \tag{2.15}$$

Combining Eqs. (2.12)–(2.15) we obtain

$$l\sim E\gamma^{-1}=Ew^{-2}L^{-d} \ , \tag{2.16}$$

which is the same as the result obtained through Born's

approximation for scattering.

In Sec. III we check numerically the range of validity of Eq. (2.16) for $d=1$. We must point out that the $d=1$ case is very unfavorable for the validity of Eq. (2.16) because, as we shall see, the small parameter w is multiplied by the unperturbed Green's function G, which in the $d=1$ case diverges near the band edge as $E^{-1/2}$.

III. NUMERICAL RESULTS

We have calculated numerically the diagonal matrix element G of the Green's function, where $G \equiv \langle m \mid (E+is-H)^{-1} \mid m \rangle$ as $s \to 0^+$. From G one obtains the density of states (DOS) per site $n(E)$ as

$$n(E) = -\frac{1}{\pi} \mathrm{Im} G \ . \tag{3.1}$$

To evaluate G numerically we have employed the so-called renormalized perturbation expansion[3] which reduces in one-dimension (1D) to an iterative procedure.[3] We have taken finite linear segments of length N up to 5000. We have generated in the computer M different sets of the random variables $\{\varepsilon_n\}$, $n=1,\ldots,N$, taken from the ensemble defined by Eq. (2.2); M was usually chosen equal to 200, but higher values were also used. We have generated the random variables $\{\varepsilon_n\}$ the following way. Once an ε_n is generated at the site n with the probability distribution given by Eq. (2.2a), the variable ε_{n+1} on the site $n+1$ has a sign opposite that at n with probability p and $(1-x)p/x$ for $\varepsilon_n = -\varepsilon/2$ and $\varepsilon/2$, respectively. This procedure ensures that the appropriate concentration x and correlation will be achieved. For each set $\{\varepsilon_n\}$ we have calculated G at the central site; we have taken s to be $8 \mid V \mid /N$, i.e., twice the average level spacing. In Figs. 1 and 2 we present some of our results for $\langle n(E) \rangle$ where $\langle\ \rangle$ denotes an average over the M members of the ensemble.

In Fig. 1 we plot the averaged $n(E)$ versus E [in units of $\mid V \mid$ for the 50-50 AB alloy ($x=0.50$)]. The middle panel corresponds to the uncorrelated case ($p=x$), the top panel gives a strongly $\ldots ABAB\ldots$ correlated case ($p=0.95$, $L=19$), and the bottom panel a strongly "phase-separated" case $\ldots AABB\ldots$ ($p=0.05$, $L=19$).

We see first that the averaged DOS exhibits the characteristic complicated structure of random binary alloys in (1D). This structure is not an artifact of the numerical approximation, but it reflects the fact that even the averaged DOS of a random one-dimensional alloy is an ill-defined function of energy. (The integral over E of the averaged DOS is a continuous but not differentiable-function.) Apart from these fluctuations the middle panel resembles that of a slightly broadened periodic case. The outward shift of each band edge is given by $1.2w^{4/3}/\mid V \mid^{1/3}$, $w^2 = 4\varepsilon^2 x(1-x) \simeq \frac{1}{16}$; in addition, barely visible tails develop.[7]

In the upper panel two subbands tend to be formed, separated by a gap at the center which is fully formed only in the limit $p=1$, where a perfect $ABAB\ldots$ ordering is established. For $p<1$ there are tails of the two subbands towards the gap; in addition, there are "defect" states (always appearing as pairs at $\pm E_0$ within the pseudogap[8]) associated with the improper joining of two normal segments, e.g., $\ldots ABA\underline{BB}ABA\ldots$.

In the bottom panel, where there is strong phase separation, the DOS can be analyzed as the superposition of two bands: the A band extending from $-1.75 \mid V \mid$ to $2.25 \mid V \mid$ and centered at $\varepsilon_A = 0.25 \mid V \mid$, and the B band extending from $-2.25 \mid V \mid$ to $1.75 \mid V \mid$. Note that the lower band at $E=-1.75 \mid V \mid$ of the upper (i.e., the A) subband is smoother than the upper band edge at $E=2.25 \mid V \mid$ of the same band. This is due to the fact that states at $E \approx 2.25 \mid V \mid$ are strongly localized since the B subband at this energy is impenetrable, while states of the A subband at $E=-1.75$ can mix with states of

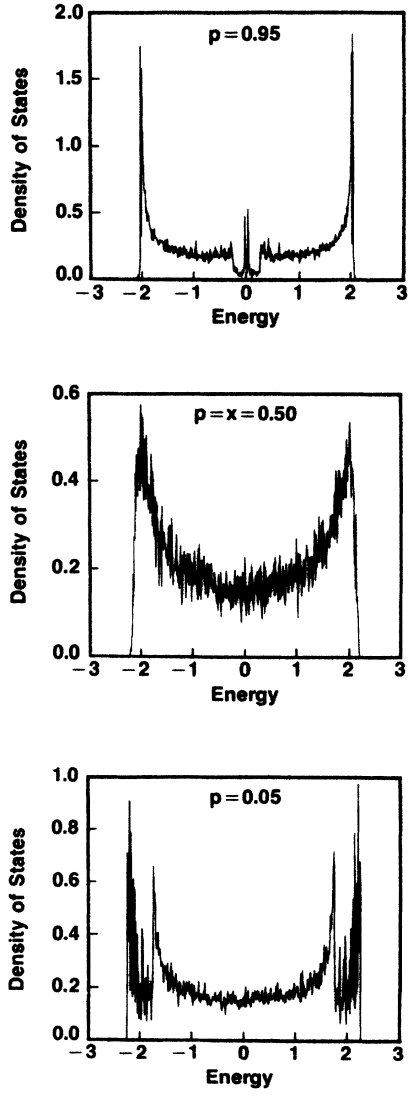

FIG. 1. Density of states per site (in units of $\mid V \mid^{-1}$) averaged over $M=200$ configurations vs energy (in units of $\mid V \mid$) for a random correlated binary alloy; x, the concentration of the A component, is 0.50 and its site energy $\varepsilon_A = 0.25 \mid V \mid$ (the B-site energy is $\varepsilon_B = -0.25 \mid V \mid$). The quantity p is the probability of a site being A under the condition that a neighboring site is B.

the B subband and thus become more extended. Similar observations can be made for the upper and the lower band edges of the B subband.

In Fig. 2 we plot the averaged $n(E)$ versus E for the $x=0.20$ case. The middle panel corresponds to the uncorrelated case $p=x$. We see that this DOS developed an asymmetry which is understandable if one thinks of the A site as repulsive impurities in a host of B sites; this repulsion tends to create a strong tail of localized states at the upper band edge as observed. The lower band is less affected by the repulsive impurity potentials. The upper panel is very similar to the middle one because, as a result of low A concentration, the AB correlation cannot be increased substantially [remember that the maximum value of p is $x/(1-x)$, i.e., equal 0.25 for $x=0.20$]. In the bottom panel, corresponding to strong

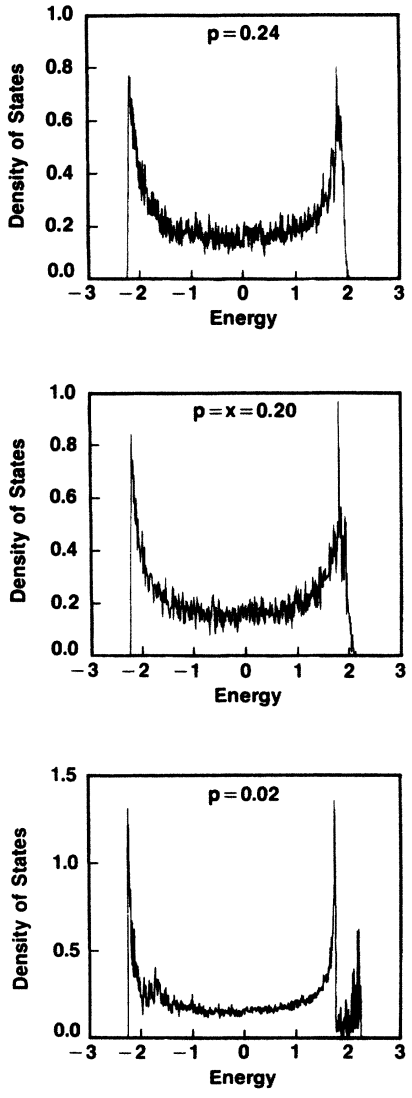

FIG. 2. Density of states per site (in units of $|V|^{-1}$) averaged over $M=200$ configurations vs energy (in units of $|V|$) for a random correlation binary alloy; x, the A component concentration, is 0.20 and its site energy $\varepsilon_A=0.25|V|$ (the B-site energy is $\varepsilon_B=-0.25|V|$). The quantity p is the probability of a site being A under the condition that a neighboring site is B.

A-B segregation (correlation length $L=19$), there are two interesting features. First, the upper tail in the middle panel has split off to create an upper part of an A pseudo gap, as expected. Second, an additional structure appears at $E\approx-1.75|V|$, where the lower band edge of an A band would be, again as expected.

In Figs. 3 and 4 we present the main results of the present study, i.e., the dependence of the localization length λ on the correlation length L, which is given by $(2x-p)/p$ for $p\leq x$ and by $p/(2x-p)$ for $p\geq x$. Again we generated numerically M sets of random variables $\{\varepsilon_n\}$ $(n=1,\ldots,N)$ according to the probability distribution (2.2). For each set we calculated numerically the transmission amplitude $\bar{t}_N$ (the transmission coefficient is $|\bar{t}_N|^2$). The localization length λ is then given by

$$\frac{1}{\lambda}=-\frac{1}{N}\langle\ln|\bar{t}_N|\rangle\ , \tag{3.2}$$

where the average was performed over the M members of the ensemble. The result is independent[9] of N as long as N is much larger than the correlation length L. However,[9] the standard deviation of $\ln|\bar{t}_N|$ over its average value behaves as $(\lambda/N)^{1/2}$ for $N\gg\lambda$ and is constant for $N\ll\lambda$. Thus from the numerical point of view more accurate results are obtained if $N\gg\lambda$.

In Fig. 3 we plot the localization length λ versus the inverse correlation length $1/L$ for the case $x=0.5$ for six different values of the energy E. In the $x=0.5$ case $\lambda(E)=\lambda(-E)$; thus we restricted ourselves to the nonpositive energies only. The following features of our results must be pointed out.

(1) For $E=-2$ (which corresponds to relatively long wavelength) the behavior is not in agreement with the QU result $\lambda=\lambda_0/L$; actually the slope $d\lambda/d(1/L)$ at $L=1$ is about $0.4\lambda_0$ instead of λ_0.

(2) For $E<-1.75$ (i.e., below the lower A band edge) and for the phase-separation case $p<x$ (left-hand side of each panel), the localization length decreases monotonically with increasing L. This is not surprising since for these energies the $AAA\ldots$ long cluster is impenetrable.

(3) For $-1.75<E<1.75$ in the long-correlation-length limit ($p\to0$; extreme left-hand side of each panel) the localization length λ increases proportionally with L. This is not surprising since the only scattering comes at the interfaces of the A and B clusters. The concentration of these interfaces is proportional to $1/L$.

(4) The slope $d\lambda/d(1/L)$ at $p=x^-$ is negative for the range of energies from $E\simeq-1.3$ to 1.3. [Note that $d(1/L)/dp=2/x$ for $p=x^-$ and $-2/x$ for $p=x^+$]. We remind the reader that the QU predicts a slope equal to λ_0, where λ_0 is the second-order perturbation result for the localization length in the absence of correlations.

(5) For E around zero (from about -0.5 and 0.4) and *for the AB case* ($x<p$) λ behaves as $\lambda=\lambda_0/L$ to a good approximation.

(6) For $\varepsilon<|E|<(2+\varepsilon^2)^{1/2}$ and for $p\to1$ the localization length increases proportionally with L. This is not surprising since the scattering centers in this case are the points where two long $ABAB\ldots$ segments are joined im-

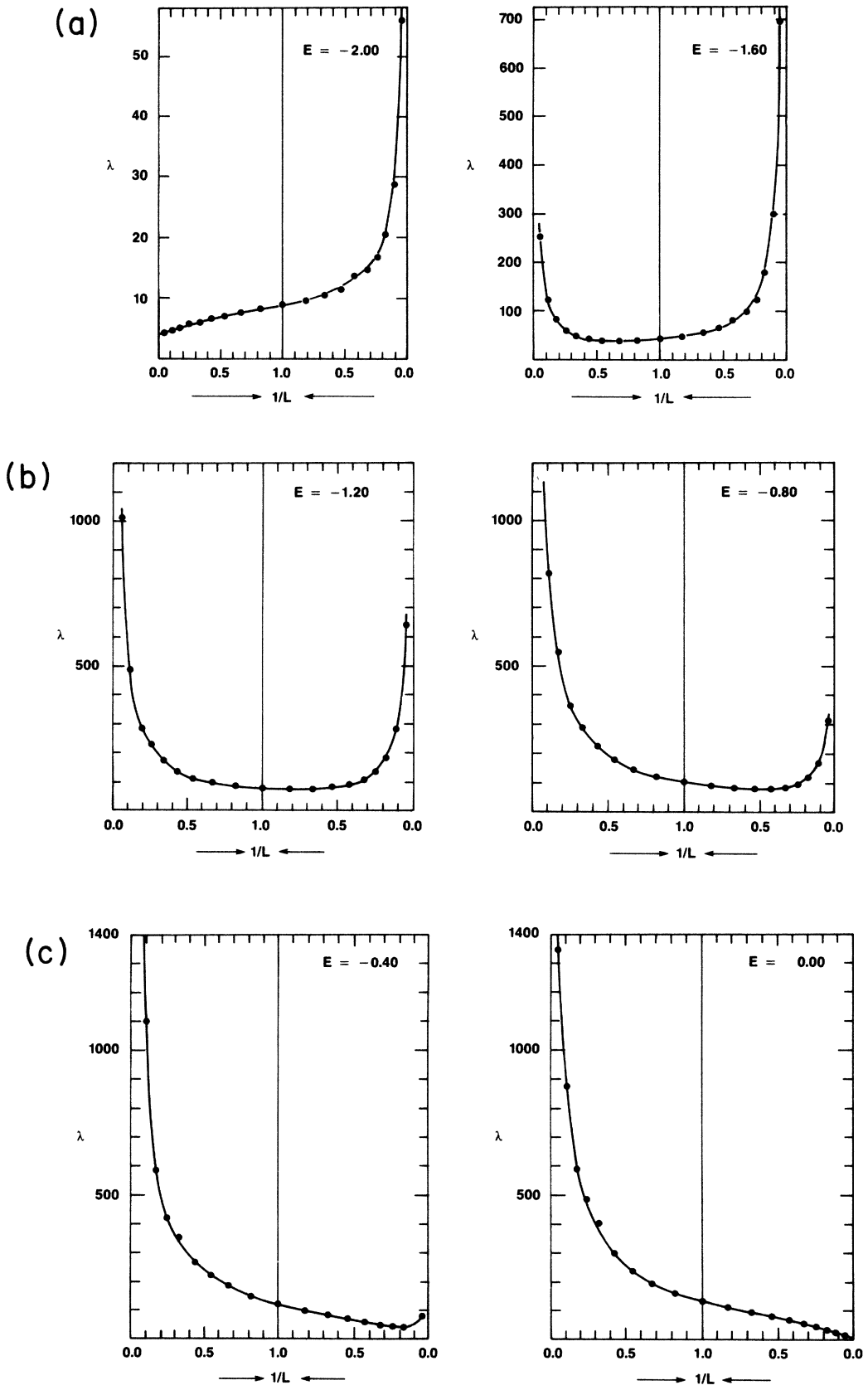

FIG. 3. Localization length λ (in units of the lattice spacing) vs inverse correlation length $1/L$ for six different values of the energy and for $x=0.5$. In each panel the left-hand half corresponds to $p<x$ [in which case $L=(2x-p)/p$] and the right-hand half to $x<p$ [in which case $L=p/(2x-p)$]. The site energies are $\varepsilon_A=-\varepsilon_B=0.25\,|V|$.

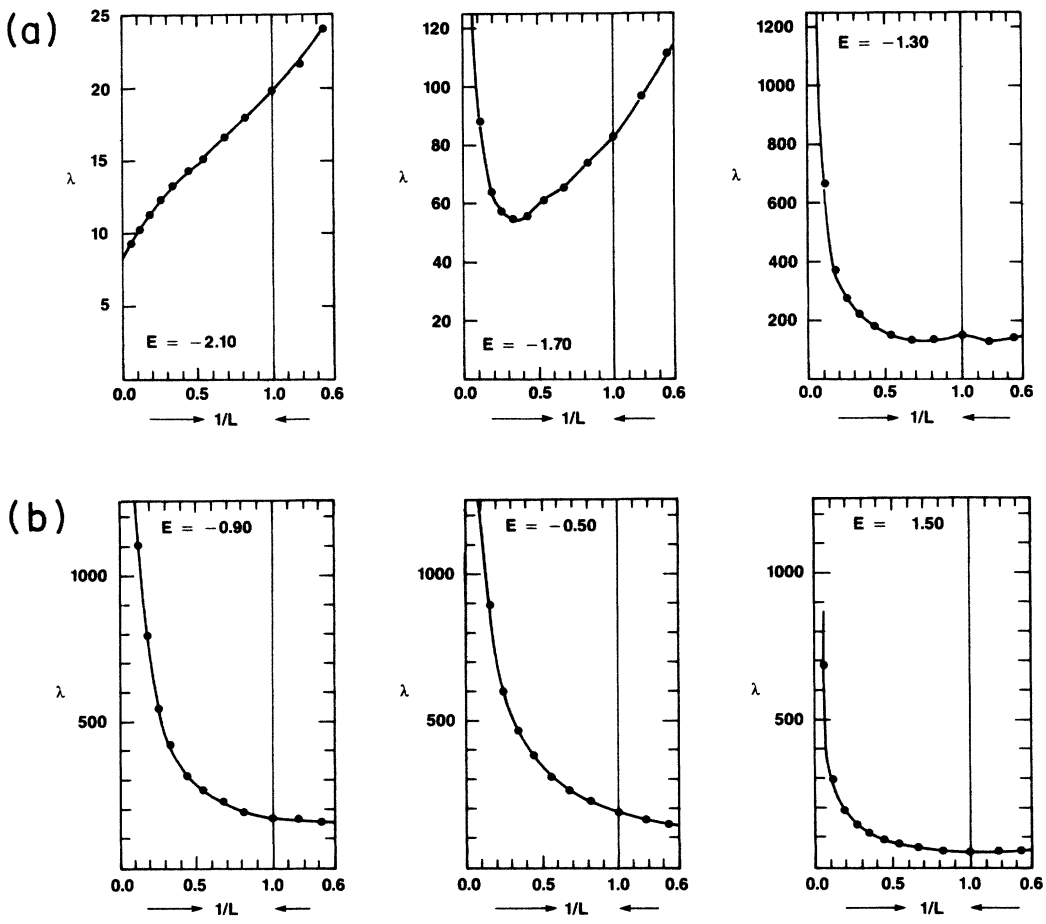

FIG. 4. Localization length λ vs inverse correlation length $1/L$ for six different values of the energy and for $x=0.5$. In each panel the left-hand side corresponds to $p<x$ segregated ordering and the the right-hand half to $x<p$ alternating ordering. The site energies are $\varepsilon_A=-\varepsilon_B=0.25\,|V|$.

properly. The concentration of such improper joinings is obviously proportional to $1/L$.

(7) For $|E|<\varepsilon$ and for $p\to 1$ the localization length decreases monotonically, which is to be expected since the region $(-\varepsilon,\varepsilon)$ defines the gap of a perfect

In Fig. 4 we plot the localization length λ versus the inverse correlation length $1/L$ both for the phase-separation case ($p<x$, left-hand side of each panel) and the $ABAB$ case ($x<p$, right-hand side of each panel). In this case p cannot exceed $0.2/0.8=0.25$ and thus the alternating ordering case has a maximum correlation length equal to 1.666.

The behavior of λ versus $1/L$ for the segregated case ($p<x$) is similar to that shown in Fig. 3. It is worthwhile to point out that $d\lambda/d(1/L)$ for $p=x^-$ remains negative for all values of E larger than about -1.3, although the $E>1.5$ the slope is very small. This was not quite expected since, when the Born approximation is valid, the behavior just inside the lower and upper band edges must be similar.

For the alternating ordering case ($x<p$) the behavior is again similar to that shown in Fig. 3. Here, however, $1/L$ cannot be less than 0.6.

IV. DISCUSSION AND COMMENTS

In this section we attempt to interpret the basic features shown in Figs. 3 and 4, i.e., the sign and possibly the magnitude of the slope $d\lambda/d(1/L)$ at $=x^-$ and the behavior as $p\to 0$ or $p\to 1$.

Let T be the t matrix corresponding to the random part of our Hamiltonian,

$$H_1=\sum_n(\varepsilon_n-\langle\varepsilon_n\rangle)\,|n\rangle\langle n|\ .$$

Then one can easily show using the relation[3] $|\psi\rangle=|\phi\rangle+GT\,|\phi\rangle$ that the transition $\bar{t}$ and the reflection r amplitudes are given by

$$\bar{t}=1+GT_f\ , \tag{4.1}$$

$$r=GT_b\ , \tag{4.2}$$

where G is the diagonal matrix element of the Green's

function for the unperturbed Hamiltonian,

$$G=-i\frac{1}{[B^2-(E-\langle\varepsilon\rangle)^2]^{1/2}}\ , \tag{4.3a}$$

$$B=2\,|\,V\,|\ . \tag{4.3b}$$

T_f and T_b are the forward and backward matrix elements of T,

$$T_f=\sum_{n,m} e^{ik(n-m)}\langle m\,|\,T\,|\,n\rangle\ , \tag{4.4}$$

$$T_b=\sum_{n,m} e^{ik(n+m)}\langle m\,|\,T\,|\,n\rangle\ , \tag{4.5}$$

$$E-\langle\varepsilon\rangle=2V\cos k\ . \tag{4.6}$$

To second order in perturbation theory we can write $T=H_1+H_1GH_1$, from which we obtain

$$\langle\,|\,T_b\,|^2\rangle=\sum_{n,m} e^{2ik(n-m)}\langle(\varepsilon_n-\langle\varepsilon\rangle)(\varepsilon_m-\langle\varepsilon\rangle)\rangle\ . \tag{4.7}$$

Combining Eq. (4.6) with Eq. (2.10), we obtain

$$\langle\,|\,T_b\,|^2\rangle\simeq Nw^2\frac{1-y^2}{1+y^2-2y\cos(2k)}+O(w^3)\ , \tag{4.8}$$

where

$$y=(x-p)/x\ . \tag{4.9}$$

Combining Eq. (4.2) and (4.8) with Eq. (3.2), which for $N\ll\lambda$ can be rewritten as

$$\frac{1}{\lambda}=\frac{1}{2N}\langle\,|\,r\,|^2\rangle\ , \tag{4.10}$$

we obtain

$$\frac{\lambda}{\lambda_0}=\frac{1+y^2-2y\cos(2k)}{1-y^2}+O(w)\ , \tag{4.11}$$

where λ_0, the second-order perturbation result for the localization length in the absence of correlations, is given by

$$\lambda_0=2/\,|\,G\,|^2w^2+O(w^3)\ . \tag{4.12}$$

The slope $d(\lambda/\lambda_0)/dp$ at $p=x$ is obtained from (4.11),

$$\frac{1}{\lambda_0}\frac{d\lambda}{dp}\bigg|_{p=x}\simeq\frac{2}{x}\cos(2k)+O(w) \tag{4.13}$$

or, equivalently,

$$\frac{1}{\lambda_0}\frac{d\lambda}{d(1/L)}\bigg|_{p=x^-}=\cos(2k)+O(w)\ , \tag{4.14}$$

which in the limit of long wavelength $k\to0$ coincides with the QU and the Born approximation, as it should.

Note that the slope given by Eq. (4.14) changes sign when $k=\pi/4$, i.e., when $|E-\langle\varepsilon\rangle|\simeq1.4\,|\,V\,|$. This value is in fair agreement with the observed energy $|E-\langle\varepsilon\rangle|\simeq1.3\,|\,V\,|$ for which the slope vanishes (see Fig. 3), and provides an interpretation of our results for smaller values of L. In particular, for $k\simeq\pi/2$, i.e., near the center of the band, Eq. (4.14) predicts a slope of -1 for $p=x^-$ and hence a slope of $+1$ for $p=x^+$, which is in very good agreement with the results shown in Fig. 3. The physical reason for obtaining the QU result at the band center for *ABAB* correlations is that the oscillations of the potential within the correlation length are matched by the oscillations in the wave function so that an *ABAB* potential at the center of the band is like an *AAAA* potential at the band edge.

It is worth pointing out that the perturbation-theory result of Eq. (4.14) works much better for the center of the band than for the band edge. The reason is that the perturbation expansion parameter is H_1G, which has a diagonal matrix element equal to $\varepsilon_nG=-i\varepsilon_n/2\,|\,V\,|\sin k$; thus as $k\to0,\pi$ (i.e., at the band edges) the expansion parameter ε_nG becomes large and the perturbation theory breaks down, while for $k\simeq\pi/2$ the expansion parameter $\varepsilon_nG\simeq-i\varepsilon_n/2\,|\,V\,|$, which is small. The conclusion is that in the present correlated one-dimensional case the optimum conditions for the validity of the QU argument near the band center and for *ABAB* correlations, while the divergence of G at the band edges severely restricts the range of applicability of the QU. It is worth pointing out that for the uncorrelated case the QU argument is valid in regions where perturbation expansion clearly fails, such as, e.g., in the tail regions where the previous work[6] has demonstrated the usefulness of QU. However, as the correlation length increases the range of validity of QU shrinks.

Equation (4.14) combined with the fact that the unperturbed band edge $E=-2$ for the $x=0.5$ case is about 0.19 inside the perturbed band edge[7] gives 0.64 for $d(\lambda/\lambda_0)/dL$ while the numerical value is about 0.4. This discrepancy is not surprising since perturbation theory is not expected to work so well near the band edge. It must be pointed out that the earlier failure of perturbation theory near the band edges is associated with the divergence of G. This divergence is peculiar to one-dimensional and two-dimensional systems in (2D the divergence is very weak) and it does not appear usually in three-dimensional systems, where perturbation theory is expected to work much better.

We note also that Eq. (4.11) gives as $p\to0$ or as $p\to1$ (for $x=0.5$) that $|\,y\,|\to1$ so that

$$\frac{\lambda}{\lambda_0}=\begin{cases}\dfrac{1-\cos(2k)}{2p} & \text{as } p\to0\ ,\\[2ex] \dfrac{1+\cos(2k)}{2(1-p)} & \text{as } p\to1\ .\end{cases} \tag{4.15}$$

(4.16)

The above expressions give the correct p dependence (as long as the energy is inside both subbands in the $p\to0$ case or in either subband in the $p\to1$ case) and reasonable quantitative agreement with the numerical data for k well inside the subbands. For example, for $E=-1.2$ and $p=0.05$, Eq. (4.15) gives $\lambda/\lambda_0=12.8$ [Eq. (4.11) gives $\lambda/\lambda_0=12.2$], while numerically $\lambda/\lambda_0\simeq12.4$. Similarly, for $E=-1.2$ and $p=0.95$ we obtain $\lambda/\lambda_0=7.2$, 6.9, and 7.76 from Eq. (4.16), Eq. (4.11), and numerical data, respectively. For $E=2.0$ and $p=0.05$ we obtain

$\lambda/\lambda_0=16.4$ and 15.6 from Eqs. (4.16) and (4.11), respectively, versus 6.2 from the numerical data. This discrepancy is again due to the failure of perturbation theory near the band edge.

For $p\to 0$ or 1 one can obtain asymptotically exact results by observing that for a propagating wave the dominant scattering mechanism comes from the improper joining of two very long ordered segments. Thus the problem is reduced to that of dilute impurities for which Eq. (3.2),

$$\frac{1}{\lambda}=-\frac{N_s}{N}\ln|\bar{t}|\ , \tag{4.17}$$

where N_s/N is the concentration (per unit length) of the scattering centers and $\bar{t}$ is the transmission amplitude from one scattering center. We examine in more detail the $p\to 0$ case for which $|\bar{t}|^2$ refers to the transmission coefficient for a steplike potential resulting from the joining of two semi-infinite A and B segments. The transmission coefficient $|\bar{t}|^2$ for this case is given by

$$|\bar{t}|^2=\frac{|(e^{ik_2}-e^{-ik_2})(e^{ik_1}-e^{-ik_2})|}{|1-e^{i(k_1+k_2)}|^2}\ , \tag{4.18}$$

where

$$E-\varepsilon_A=2V\cos k_1\ , \tag{4.19a}$$

$$E-\varepsilon_B=2V\cos k_2\ . \tag{4.19b}$$

Equation (4.18) is valid when both k_1 and k_2 are real, i.e., when E is within both the A and the B bands. If E is outside the one band and inside the other, then within the impenetrable segments the eigenfunction decays with a characteristic length given by $\{\cosh^{-1}[(E-\varepsilon_\alpha)/2V]\}^{-1}$, while in the penetrable ones it does not decay. Thus the localization length is given by

$$\frac{1}{\lambda}=x_\alpha\cosh^{-1}[(E-\varepsilon_\alpha)/2V]\ , \tag{4.20}$$

where $\alpha=A$ or B refers to the impenetrable species.

The concentration N_s/N of the improper joinings is given by $2(1-x)p$, so that

$$\frac{1}{\lambda}=2(1-x)p\ln|\bar{t}| \tag{4.21a}$$

$$=2(1-x)(2x-p)\ln|\bar{t}|\,\frac{1}{L}\ , \tag{4.21b}$$

for $p\to 0$ and E inside both bands. Equation (4.21) is in good agreement with the numerical data. For example, for $E=-1.6$, $\varepsilon=0.25$, $x=0.5$, and $p=0.05$ we obtain $\lambda=255$, versus 253 ± 3 from the numerical data. Similarly, for $E=-1.7$, $\varepsilon=0.25$, $x=0.2$, and $p=0.02$ we obtain 167, versus 164 ± 4 from the numerical data. In a similar way, one may analyze the $p\to 1$ case. Thus the behavior exhibited is quantitatively accountable. As we have pointed out already the behavior for short correlation lengths (comparable to the interatomic distance) is qualitatively explainable by perturbation theory although the latter is inadequate for predicting the quantitative features near the band edge even for relatively weak disorder.

In the dilute limit ($x\to 0$) one can avoid perturbation theory and analyze the problem in terms of scattering of A clusters embedded to the B matrix. If $|r_n|^2$ is the reflection coefficient from an isolated cluster containing n consecutive A sites and C_n is the number of such clusters per unit length, then from Eq. (4.10) we have

$$\frac{1}{\lambda}=\tfrac{1}{2}\sum_{n=1}^{\infty}C_n|r_n|^2\ , \tag{4.22}$$

where C_n is given by

$$C_n=x\bar{p}^{\,2}(1-p)^{n-1}\ , \tag{4.23}$$

where $\bar{p}=p(1-x)/x$ is $p_{B/A}$. In the limit $x\to 0$, Eq. (4.22) gives, for $d(\lambda/\lambda_0)/dp$ at $p=x$,

$$\frac{1}{\lambda}\frac{d\lambda}{dp}\bigg|_{p=x}=\frac{1}{x}\left[\left|\frac{r_2}{r_1}\right|^2-2\right],\quad x\to 0 \tag{4.24a}$$

or

$$\frac{1}{\lambda}\frac{d\lambda}{d(1/L)}\bigg|_{p=x^-}=\frac{1}{2}\left[\left|\frac{r_2}{r_1}\right|^2-2\right],\quad x\to 0\ . \tag{4.24b}$$

It follows from Eq. (4.2) that $r_2/r_1=T_{b2}/T_{b1}$, which can be written by using (4.5) and results from Ref. 3 as

$$\frac{r_2}{r_1}=f(1+e^{2ik}+2tGe^{2ik})\ , \tag{4.25}$$

where

$$t=\frac{\varepsilon_A-\varepsilon_B}{1-(\varepsilon_A-\varepsilon_B)G}\ , \tag{4.26}$$

$$f=(1-t^2G^2e^{2ik})^{-1}\ . \tag{4.27}$$

In obtaining Eqs. (4.26) and (4.27) we have used the relation[3] $\langle l|G|m\rangle=Ge^{ik|l-m|}$. For $\varepsilon\to 0$, Eqs. (4.26) and (4.27) give

$$\frac{r_2}{r_1}=1+e^{2ik}+O(\varepsilon)\ , \tag{4.28}$$

which, combined with (4.24), recaptures the perturbation result of Eqs. (4.13) and (4.14).

In Fig. 5 we plot $|r_2/r_1|^2$ versus $E-\varepsilon_B$ as obtained from Eqs. (4.25)–(4.27) for $\varepsilon_A-\varepsilon_B=0.5|V|$, together with the perturbation result of $2+2\cos(2k)$. Note that the symmetry around $E-\varepsilon_B=0$ for the perturbation result is broken and that $|r_2/r_1|^2$ is less than 2 near the upper band edge. Thus the slope $d\lambda/dp$ is negative there, in agreement with the results shown in Fig. 4(b). Actually, $|r_2/r_1|^2$ is larger than 2 only in a rather narrower region $-1.90<E+0.25<-0.95$ in which $d\lambda/dp$ is expected to be positive. This agrees with the data of Fig. 4(a). The values of the slope $(d\lambda/\lambda_0)/dp$ at $E=-2.10$ and -1.70 obtained from the limiting equation (4.24a) are 2.25 and 4.25, respectively. The corresponding numerical values (for $x=0.20$) are 4.6 and 5.5.

The observed symmetry between the upper and lower band edges can be understood as follows: the A impuri-

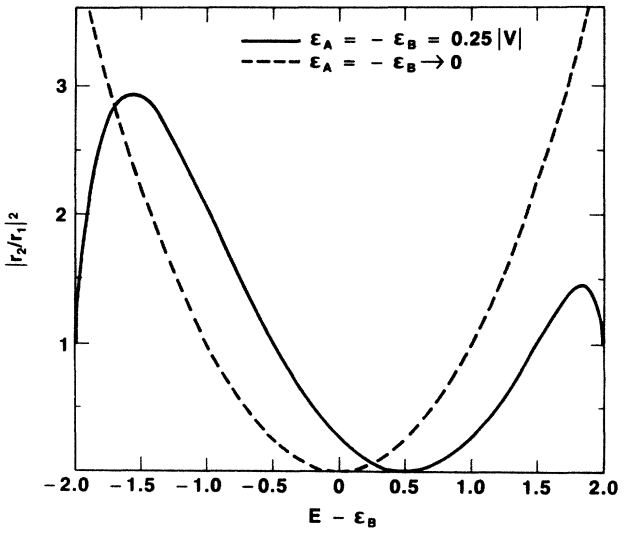

FIG. 5. Plot of $|r_2/r_1|^2$ vs $E-\varepsilon_B$ (in units of $|V|$), where $|r_2|^2$ ($|r_1|^2$) is the reflection coefficient from two (one) consecutive A sites embedded in an infinite B medium.

ties in a B host represent a repulsive scattering potential, but a repulsive potential at the upper band edge is equivalent to an attractive potential at the lower band edge. Thus the asymmetry tails us that an attractive potential is a more effective scatterer than an equal strength repulsive potential (for positive effective mass). That this is so can be seen from either perturbation theory[10] or from the fact that an attractive potential exhibits resonances whereas a repulsive one does not.

V. CONCLUSIONS

We have studied a tight-binding model of a correlated random one-dimensional binary alloy. Our purpose was to check the range of validity of the quasiuniversality (QU) approach and to examine the effects of the correlation. It must be pointed out that long correlation lengths allow us to map the problem to that of wave propagation in the continuum. The latter is directly related to the interesting question of light localization.[10–13]

We found that QU holds near the center of the band for alternating $ABAB$ correlation. It is also valid near the band edge for the phase-separation correlation, but only for very weak disorder. As the disorder increases the perturbation expansion and the QU break down prematurely due to the fact that the unperturbed Green's function increase in size near the band edge in 1D.

Increasing the correlation length may decrease or increase localization depending on the type of correlation, on the energy, on the disorder, on the concentration, and on the size of the correlation length. For phase-separation correlation and near the band edge, but above the lower A band edge, an increase of the correlation length initially decreases the localization length until a minimum is reached beyond which the localization length increases again. The search for the conditions for making this minimum lower is very interesting because the minimum is related to whether optical localization appears in three-dimensional systems.[14]

*Permanent address: Department of Physics and Ames Laboratory, Iowa State University, Ames, IA 50011.

[1]N. F. Mott and E. A. Davies, *Electronic Processes in Non-Crystalline Materials*, 2nd ed. (Clarendon, Oxford, 1979),

[2]P. A. Lee and T. V. Ramakrishnan, Rev. Mod. Phys. **57**, 287 (1985).

[3]See, e.g., E. N. Economou, *Green's Functions in Quantum Physics*, 2nd ed. (Springer-Verlag, Heidelberg, 1983).

[4]See, e.g., *Excitations in Disordered Systems*, edited by M. F Thorpe (Plenum, New York, 1981).

[5]E. N. Economou, C. T. White, and R. DeMarco, Phys. Rev. B **18**, 3946 (1978).

[6]M. H. Cohen, E. N. Economou, and C. M. Soukoulis, Phys. Rev. B **32**, 8268 (1985).

[7]E. N. Economou, C. M. Soukoulis, M. H. Cohen, and A. D. Zdetsis, Phys. Rev. B **31**, 6172 (1985).

[8]E. N. Economou and Paul Mihas, J. Phys. C **10**, 5017 (1977).

[9]A. A. Abrikosov, Solid State Commun. **37**, 997 (1981).

[10]L. D. Landau and E. M. Lifshitz, *Quantum Mechanics*, 2nd ed. (Pergamon, New York, 1965), p. 486.

[11]S. John, Phys. Rev. Lett. **53**, 2169 (1984).

[12]P. W. Anderson, Philos. Mag. B **52**, 505 (1985).

[13]P. Sheng and Z.-Q. Zhang, Phys. Rev. Lett. **57**, 1879 (1986).

[14]E. N. Economou, C. M. Soukoulis, and M. H. Cohen (unpublished).